

Optimal Design of 3-phase Squirrel Cage Induction Motors Using Genetic Algorithm Based on the Motor Efficiency and Economic Evaluation of the optimal Model

M. REZAIIEE NAKHAEI, R. ROSHANFEKR


Abstract— There are different approaches to improve the efficiency of induction motors. In this paper, the considered approaches include, design of the rotor slot, rotor slot shape, and stator and rotor diameters which are applied on a 30-kW 3-phase, 4-poles, 48-stator slots, and 44-rotor squirrel cage induction motor. Comparison of analytical, simulation and experimental results confirm the proposed finite element method (FEM) based model of set-up induction motor. The sensitivity analysis of efficiency considering the variations of rotor slot dimensions, stator outer diameter, and stator and rotor diameters have been applied on the case-study. The results of the genetic algorithm (GA) based optimal design of the rotor slot dimensions showed a 0.32% improvement in motor efficiency. On the other hand, changing the motor core diameters has more effects on motor efficiency so that, when the stator and rotor outer diameters were increased simultaneously, the efficiency was increased by 0.55%. However, if the stator outer diameter just increased, motor efficiency increased by 0.76%. Finally, the economic evaluation was accomplished to validate the optimal approach of motor design for three cases of electricity consumption per kWh.

Index Terms— squirrel cage induction motor, geometric dimension, efficiency, optimization, economic evaluation


I. INTRODUCTION

THE SQUIRREL cage induction motors are extensively used in many industrial fields and home applications because of their simple structure, reliability, low cost, robustness, less maintenance and ability to work in inimical

MAHDI REZAIIEE NAKHAEI, is with Department of Electrical Engineering University of Hakim Sabzevari, Sabzevar, Iran, (e-mail: mehdiRezaei24@yahoo.com).

 <https://orcid.org/0000-0002-1008-2180>

REZA ROSHANFEKR, is with Department of Electrical Engineering University of Hakim Sabzevari, Sabzevar, Iran, (e-mail: r.roshanfekr@hsu.ac.ir). Corresponding Author

 <https://orcid.org/0000-0002-6442-1571>

Manuscript received May 06, 2020; accepted January 05, 2021.

DOI: [10.17694/bajece.732721](https://doi.org/10.17694/bajece.732721)

environments. Since the starting torque in an induction motor is poor, there is a limitation to be used in some applications requiring high starting torque. One of the ways to increase the starting torque is adjusting the resistance and reactance of the rotor, especially the upper part of rotor slot resistance according to the skin effect in the motor startup. To reach this goal, it is necessary to design the rotor bars of the squirrel cage induction motor. The slot depth design is another procedure to improve the starting torque however, this design increases rotor slot leakage reactance and decreases motor efficiency [1-3].

Besides the low starting torque by induction motors, the efficiency of these motors should pay particular attention due to the wide applications in industry. According to the results of an investigation for the United State Federal Energy Administration, the electric motors consume 64% of the total electric consumption in the United-state. Thus, energy conservation requires focusing on electric motors, and their efficiencies [4, 5].

Many previous studies for increasing starting torque, efficiency, and power factor in induction motors have been carried out for a long time. As the rotor bar shape has more important effects on motor performance characteristics, there are many studies about rotor bar design. In some studies, to increase starting torque and efficiency or achieve a certain torque-speed curve, the rotor slot shape has been changed [1, 3-7]. In the other studies, the motor characteristics have been changed by using ways of adjusting slot dimensions and rotor slot area whereas the shape of the rotor slot has been maintained [8-11].

Besides, the aluminum die-cast is the way to fill the rotor bars and end rings. In this process, the porosity phenomena in bars and end rings of the rotor can occur. The porosity is proportional to the fill factor reversely. The results show that efficiency and starting torque will be increased by 1.92 %, and 11.93 %, whereas the fill factor is adjusted from 62% to 93%, respectively [12, 13]. But, in the industry, the fill factor is usually over 96 % and also it is difficult to model in software design.

The skewed rotor bars are employed to reduce the harmonic components of motor specifications. For instance, the total harmonic distortion (THD) of stator current with and without

the skewed model is 0.9% and 1.61%, respectively [14]. So, the skewed rotor has a significant effect on harmonic components. The novel skewed rotor presented in [15], decreases the radial electromagnetic force as well as the harmonics flux density amplitude for radial, circumferential, and axial component. Also, the noise of the motor in the improvement model is reduced.

The inclination of rotor bars which is different from the skewing of rotor bars has a significant effect on efficiency so that it is increased by 0.63% whereas the starting torque is increased only 0.63 % when the inclination angle adjusted from 0° to 25° [16]. However, the rotor bar inclination is limited when the number of rotor slots increases.

In the primary design of the induction motor, when the design process leads to lower efficiency than the desired value, the increase stator core is the way to increase efficiency [17, 18]. The stack length is one of the motor geometry parameters which was considered by [19] so that when the stack length is increased in different commercially manufactured induction motors, the efficiency is increased.

When using the material with a lower loss for core laminates and conductors, the efficiency has been increased. However, the selection of laminate and conductor material has been limited, and also it increases motor costs [20].

Generally, electricity generation is expensive for every government. With the high growth rate of electrical energy consumption, it is necessary to construct more power plants. Thus, this leads to an increase in the costs and pollution of the environment. To reduce the energy consumption with the industrial induction motors, the main goal of this article is the optimal efficiency design of 3-phase squirrel cage induction motors.

In this article, based on the mathematical equations related to geometric dimensions of induction motors, the motor performance characteristics have been determined. The motor performance results obtained from mathematical equations, model simulation using RMXprt-Maxwell software and experimental tests applied to a 30-kW 4-pole 3-phase squirrel cage induction motor have been compared. Also, different approaches with combination of the genetic algorithm have been applied to the model of the set-up motor as the conventional model to improve the motor efficiency. Finally, the economic evaluation of the optimal model has been considered to validate the optimal motor design approach.

II. ANALYTICAL BACKGROUND

The performance characteristics of induction motors are determined according to their geometric dimensions. In this section, the mathematical equations related to the motor efficiency and power factor are described in which they are proportional to the motor equivalent circuit [21]. The details of these equations have been presented in [22].

The Efficiency (η) is proportional to losses so that can be expressed using Eq. (1):

$$\eta = P_{out} / (P_{out} + P_{loss}) \quad (1)$$

where, P_{out} is rated output power, and P_{loss} is power losses of motor. The induction motor losses can be divided into the iron loss, stator copper loss, rotor copper loss, mechanical loss, and stray loss:

$$P_{loss} = P_{iron} + P_s + P_r + P_m + P_{stray} \quad (2)$$

where P_m is mechanical loss, P_{stray} is stray loss.

The stator copper loss depends on the resistance of stator (R_s) and motor rated current (I_n):

$$P_s = 3R_s I_n^2 \quad (3)$$

Similarly, the rotor copper loss can be described as:

$$P_r = 3(R_r)_{S_n} I_m^2 = 3R_r K_I^2 I_n^2 \quad (4)$$

where R_r is the resistance of rotor in the rated speed, I_n is rated current, and K_I is coefficient of stiffness stator mmf relative to the rotor.

The core loss P_{iron} consists of the fundamental P_{iron}^l and harmonic P_{iron}^h iron loss. The fundamental iron loss occurs only in the stator teeth (P_t^l) and stator yoke (P_y^l) due to the rotor frequency is low. The stator teeth fundamental loss P_t^l and the stator yoke fundamental loss P_y^l can be calculated approximately using Eq. (5) and (6):

$$P_t^l \approx K_t \times P_1 \times (f_1 / 50)^{1.3} B_{ts}^{1.7} G_{ts} \quad (5)$$

$$P_y^l \approx K_t \times P_1 \times (f_1 / 50)^{1.3} B_{ys}^{1.7} G_{ys} \quad (6)$$

where P_1 is specific losses in W/Kg at 1.0 Tesla and 50Hz, K_t is coefficient core loss augmentation due to the mechanical machining, f_1 is the fundamental frequency, G_{ts} is stator tooth weight, G_{ys} is stator yoke weight, B_{ts} is tooth flux density, and B_{ys} is yoke flux density.

Also, the harmonics iron loss P_{iron}^h includes both stator (P_s^h) and rotor (P_r^h) harmonic losses.

$$P_s^h \approx 0.05 \times 10^{-3} \cdot [(N_s (f_1 / p)(1 / (2.2 - B_{ts}))(K_{c2} - 1)B_g]^2 G_{ts} \quad (7)$$

$$P_r^h \approx 0.05 \times 10^{-3} \cdot [(N_r (f_1 / p)(1 / (2.2 - B_{tr}))(K_{c2} - 1)B_g]^2 G_{tr} \quad (8)$$

where B_g is air-gap flux density, N_s is number stator slot, K_{c2} is stator carter coefficient, K_{c1} is rotor carter coefficient, N_r is number rotor slot, and G_{tr} is rotor tooth weight.

In general, the power factor can be expressed using Eq. (9):

$$\cos \varphi = P_{out} / \sqrt{3} V_{ph} I_n \eta \quad (9)$$

where V_{ph} is phase voltage.

III. CASE STUDY

In this article, the case study is a 3-phase squirrel cage induction motor which consists of 4-pole, 48-stator slots, and 44-rotor slots with 30 kW rated power, 1474 rpm, and 380V. The outer diameter of the stator and rotor is 327 mm, and 210 mm, respectively and the core length of the motor is 230 mm. Also, the depth of stator and rotor slots are 26.8 and 38 mm, respectively.

Figure 1 shows the cross-section of the stator and rotor core. As shown in Fig. 1, the slot of the rotor is a half-slot type.

Also, the skewed rotor slot (3.48 degree) is employed to reduce the noise of motor as well as the harmonic components of motor performance characteristics.

According to the theoretical equations given in section II and motor geometrical dimensions, the performance characteristics of the set-up induction motor have been calculated. Also, the set-up induction motor as the conventional model has been simulated by RMxpert-Maxwell software based on the finite element method (FEM) [23]. The results of theoretical analysis, experimental test, and simulation applied on the conventional model have been presented in Table 1 where PF is the power factor, P_T is total losses, and T_m is maximum torque.

The experimental results presented in Table 1 have been performed in the evaluation and quality control section of Jovein Electrical Machines Industries Company (JEMCO). The purpose of this study is to improve the performance characteristics, especially the efficiency of the case study induction motor manufactured by JEMCO.

The determined performance characteristics given in Table 1, are relatively close to each other, except P_{iron} , η , P_s , and P_r . So that, the efficiency obtained from theoretical equations and experimental results is 91.14% and 91.52% respectively, however, it is 93.59 % by simulation results. The reason for the difference between these values in motor efficiency is the iron loss. The coefficient iron loss augmentation (K_i) due to the mechanical machining is considered in (5) and (6) to calculate the iron loss. Also, the opinion of professional engineers in the field of electric motor manufacturing is that the iron loss affected by mechanical machining becomes almost doubles. So, the efficiency obtained from software can be modified considering the K_i coefficient. Also, stator and rotor losses (P_s and P_r) in simulation and theory are different from experimental results. The fill factor of the squirrel cage induction motor rotor bars in the software is considered to be 100%, while in reality this coefficient is not 100%. In stator windings, in fact, the presence of stator slot insulations, the presence of wooden or plastic wedges at the top of the stator slot, and finally the end connection of the stator windings are reasons of a difference in the stator copper losses compared to the simulation that hasn't these cases.

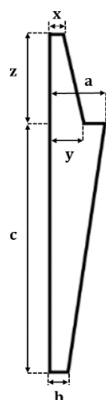


Fig.2. Rotor slot shape of the conventional induction motor

IV. SENSITIVITY ANALYSIS

In this section, the effects of rotor slot dimensions and the stator and rotor diameters on performance characteristics of the 30-kW induction set-up motor are analyzed. The result of sensitivity analysis is useful to choose a design method with appropriate variables and concentrates.

TABLE I
THE INDUCTION MOTOR PERFORMANCE CHARACTERISTICS OBTAINED FROM THEORETICAL ANALYSIS, EXPERIMENTAL TEST, AND SIMULATION RESULTS

Characteristics	Theoretical	Experimental	Simulation
P_{out} (kW)	30	30	29.99
V_{ph} (V)	380	380	380
I_n (A)	54.23	57.359	53.62
I_{start} (A)	230.21	226.65	234.22
speed (rpm)	1474	1474.31	1476
PF	0.92	0.871	0.90
P_{iron} (W)	1244	965	454.92
P_s (W)	742.8	909	770.77
P_r (W)	335.6	564	315.66
P_T (kW)	2.8	2.95	2.1
η (%)	91.14	91.518	93.59
f (Hz)	50	50	50
T_s (N.m)	330.36	482.4	339.82

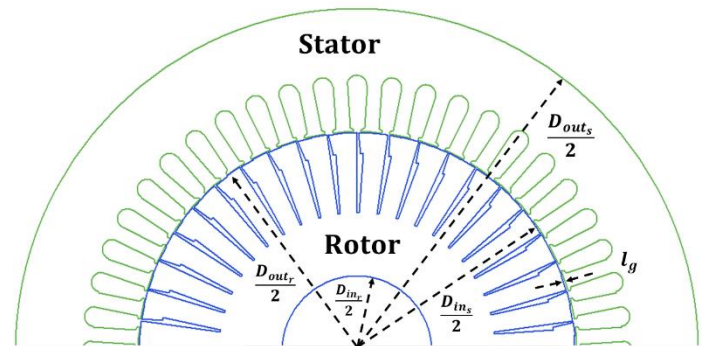


Fig.1. Cross-section of stator and rotor core related to the conventional model

A. Rotor slot dimensions

Since the induction motor is influenced by the skin effect at motor startup conditions, the current is concentrated in the upper part of the slot. Furthermore, at the motor rated conditions, the current flows of the whole slot. Hence various parts of slot and their area have effects on the performance characteristics of the motor. In this section, the effects of changing the values of the rotor slot dimensions along both width and depth are investigated on the motor efficiency, power factor and starting torque.

When each dimension of the rotor slot includes x , y , z , a , b , and c -dimension (Fig. 2) is changed, the area of the slot is no longer equal to the previous value. The current density of the rotor slot is changed when the area is changed. Due to current density variation, the rotor copper loss is changed as well as the motor efficiency. The conventional model efficiency is 93.59% refer to Table 1. The motor efficiency, power factor, and starting torque versus width and depth dimensions of the rotor slot are illustrated in Fig. 3, and Fig. 4, respectively.

Based on Fig 3-a, each part of the slot widths has a different

effect on motor efficiency so that the top part of the rotor slot width has no significant effect on efficiency. When the middle part width of the rotor slot is changed from 2mm to 12mm, the efficiency increases by 0.3%. Also, increasing the bottom part width results in a sharper decrease in motor efficiency in comparison with other parts.

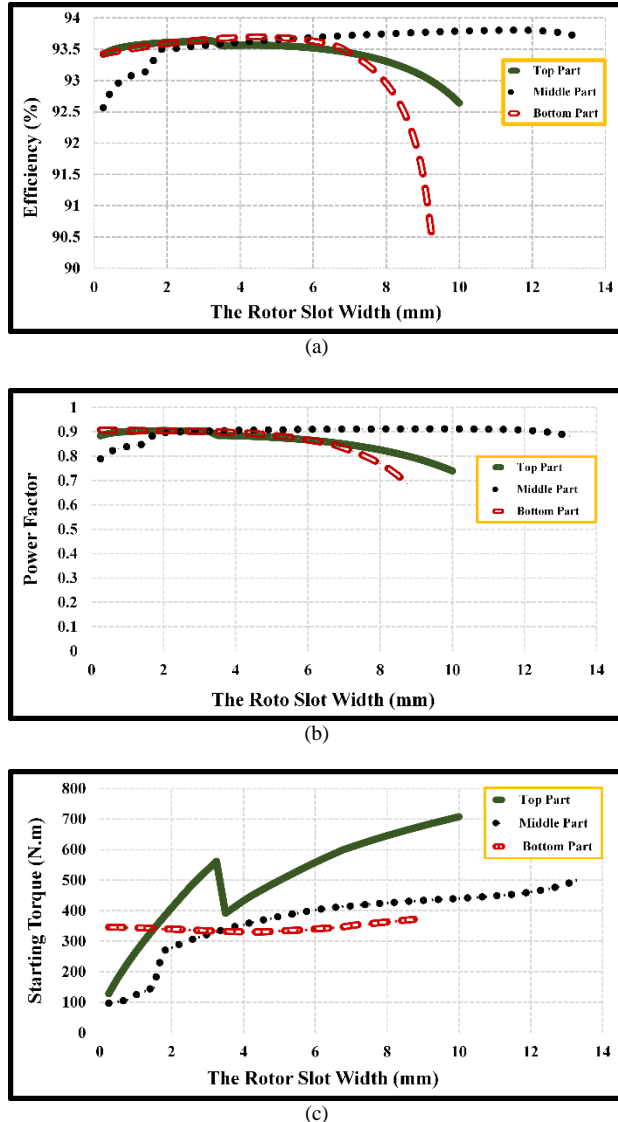


Fig.3. Different part sensitivity of the rotor slot width on performance characteristics of the conventional model. (a)- Efficiency, (b)- Power Factor, (c)- Starting torque

Figure 3-b showed that the power factor is changed similar to efficiency. Also, the starting torque has different behavior against changing the different parts of the rotor slot width. The bottom part changing does not affect starting torque due to that the current is concentrated in the top part of the rotor slot. Hence, as shown in Fig. 3-c, the top part of the rotor slot has a great effect on starting torque whereas the top part width increases from 0.25mm to 10mm, the starting torque is increased by 483%. However, the efficiency is reduced amount of 0.96%.

According to Fig. 4-a, the efficiency related to the top part

of the rotor slot depth is almost constant. However, when the bottom part depth is increased from 0.25mm to 40mm, the efficiency was increased by 4%. The variations of the power factor have been depicted in Fig.4-b which is similar to the efficiency variations, but the starting torque is decreased when the top and bottom parts depth dimensions of the rotor slot are increased as shown in Fig. 4-c.

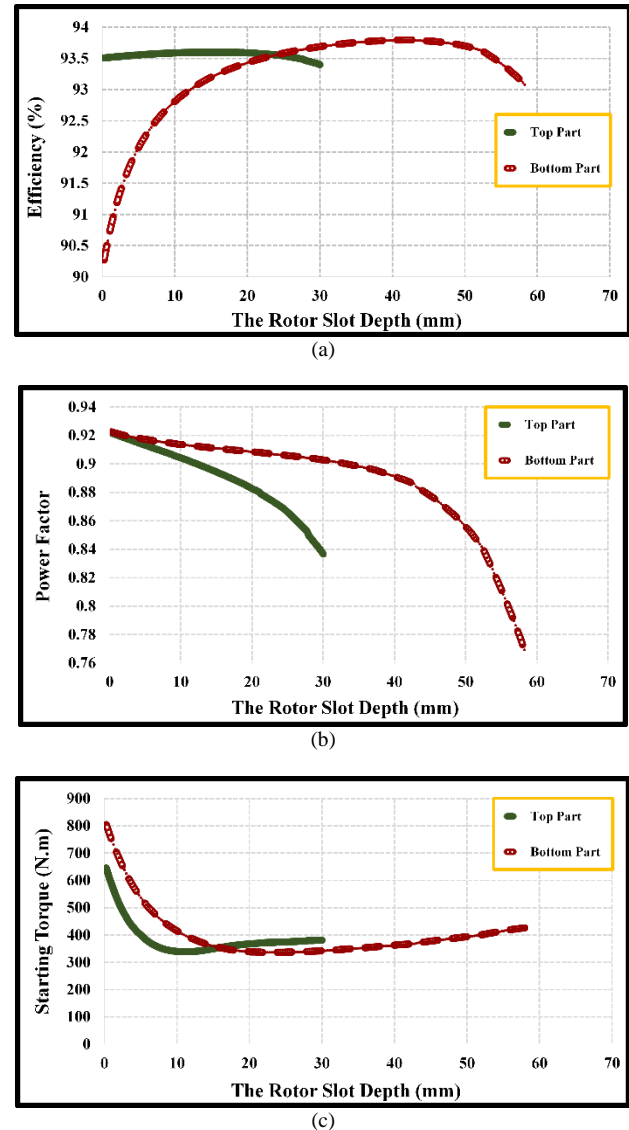


Fig.4. Different part sensitivity of the rotor slot depth on performance characteristics of the conventional model. (a)- Efficiency, (b)- Power Factor, (c)- Starting torque

Thus, all dimensions of the rotor slots have effects on the performance characteristics of the motor. It is needed a trade-off between different parts of the rotor slot (width and depth) to achieve an acceptable performance characteristic. So, a trade-off between efficiency, power factor, and starting torque is needed to choose the optimal point for D_{out-s} , D_{in-s} , D_{out-r} , and D_{in-r} .

B. Stator and rotor diameters

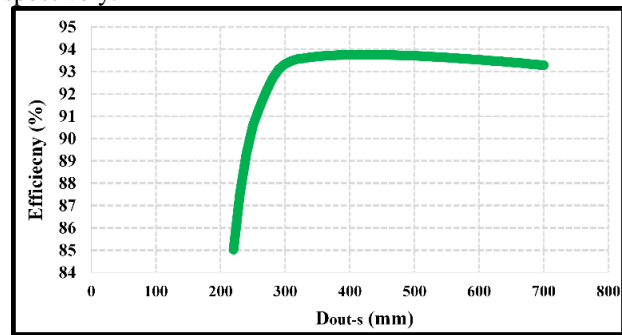
The stator inner diameter (D_{in-s}) is proportional to the ratio, which is defined as the ratio (K_D) of D_{in-s} to D_{out-s} (stator inner diameter). This ratio depends on the number of motor pole pairs (p). When the D_{out-s} is changed, the stator inner diameter, rotor outer diameter (D_{out-r}) and rotor inner diameter (D_{in-r}) can be calculated using Eq. (10)- (12):

$$D_{in-s} = K_D D_{out-s} \quad (10)$$

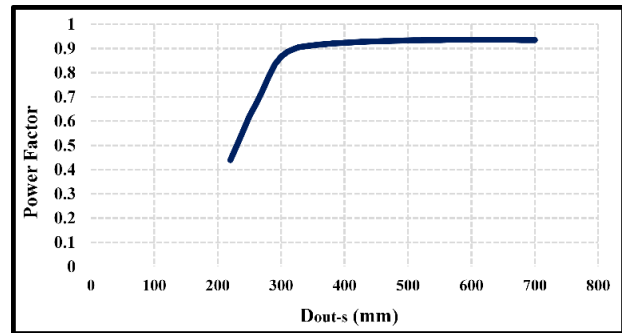
$$D_{out-r} = D_{in-s} - 2l_g \quad (11)$$

$$D_{in-r} = D_{out-r} - 2l_{slot} \quad (12)$$

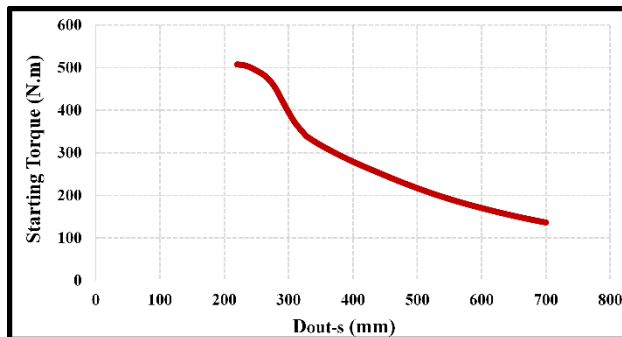
where l_g and l_{slot} are air-gap length and rotor slot depth, respectively.



(a)



(b)



(c)

Fig.5. Sensitivity of the stator and rotor diameters simultaneously on performance characteristics of the conventional model. (a)- Efficiency, (b)- Power Factor, (c)- Starting torque

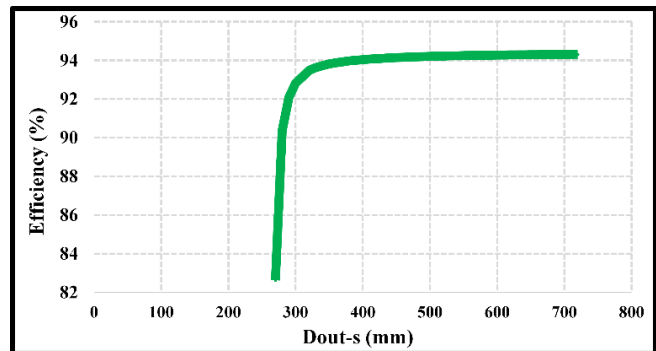
Based on the number of pole pairs in the conventional model ($p = 2$), K_D is considered 0.62. In this approach, since the stator outer diameter has been changed from 220 mm to 700 mm, also the air-gap length is 0.65mm, the D_{in-s} , D_{out-r} , have been changed from 136.4mm to 446.4, 135.1mm to

445.1mm, respectively.

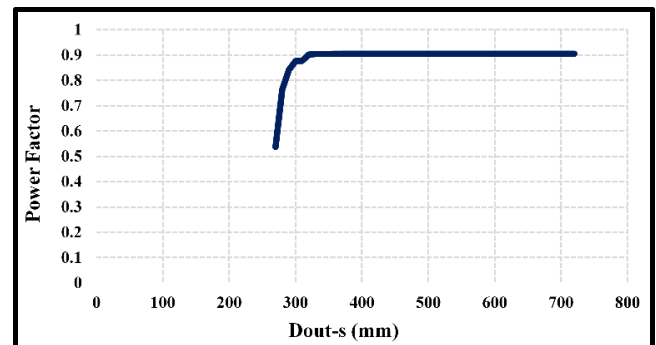
The motor efficiency, power factor, and starting torque curve versus the stator and rotor diameters at the same time is depicted in Fig. 5. Although the enlargement of core diameter increases the motor efficiency, however the starting torque reduces. The power factor is changed similar to the efficiency curve.

C. Stator outer diameter

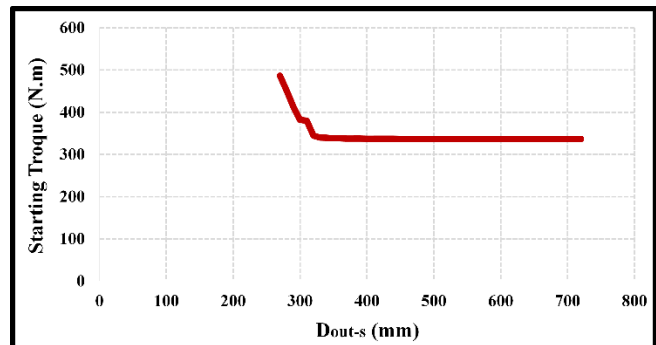
In this approach, the inner and outer diameters of the rotor and the inner diameter of the stator are constant at their initial values. The stator outer diameter is changed to analyze the effect of this variation on motor performance characteristics. The stator outer diameter has been changed from 270mm to 720mm. The efficiency, power factor, and starting torque curves versus the stator outer diameter (D_{out-s}) are depicted in Fig. 6.



(a)



(b)



(c)

Fig.6. Sensitivity of the stator outer diameters on performance characteristics of the conventional model. (a)- Efficiency, (b)- Power Factor, (c)- Starting torque

The results show that power factor and starting torque are constant when the D_{out-s} is larger than 350mm whereas efficiency is increased. However, in comparison with Fig. 5, the efficiency and starting torque decrease whereas the power factor increases.

V. APPROACHES OF MOTOR DESIGN

There are different approaches to improve the performance characteristics of induction motors. In this article, the approaches include design of rotor slot, rotor slot shape, stator and rotor diameters, and stator outer diameter are applied to the conventional model presented in section 3. The sensitivity analysis of rotor slot dimensions and stator and rotor diameters is accomplished. The genetic algorithm (GA) is employed to find the optimal geometric parameters in the proposed approaches according to the sensitivity analysis results.

A. Approach 1: Design of rotor slot

In this approach, the goal is to design an optimal rotor slot based on the rotor slot shape of the conventional model. The maximum motor efficiency has been chosen as the objective function. The optimization algorithm has six variables such as x, z, y, a, c, b which are dimensions of conventional model rotor slot (Fig. 2). The results of the GA optimization are presented in Table 2. The optimal rotor slot shape using GA is depicted in Fig. 7-b.

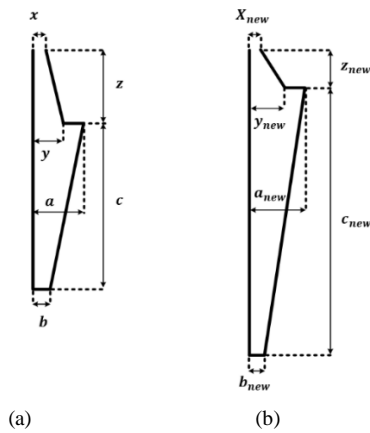


Fig.7. Rotor slot shape. (a)- Conventional model, (b)- Optimal model related to the approach 3

TABLE II
THE RESULTS OF GA OPTIMIZATION

Variables	Limit (mm)	Initial value (mm)	optimal value (mm)
x (mm)	0.75-2.25	1.5	1.509
z (mm)	5-15	10	5.900
y (mm)	1.75-5.25	3.5	4.605
a (mm)	2.9-8.7	5.8	7.876
c (mm)	14-42	28	38.039
b (mm)	1-3	2	1.549

The simulated performance characteristics of the optimal motor have been presented in Table 3. The results show that the optimal motor efficiency in this approach increases by 0.32% in comparison with the conventional motor efficiency. Besides, the starting torque increases by 18.13%, as well as the starting current by 31.36% in comparison with the

conventional model. Furthermore, the PF of the optimal decreases by 0.55% in comparison with the conventional motor PF.

TABLE III
THE INDUCTION MOTOR CHARACTERISTICS OF THE OPTIMAL ROTOR SLOT SHAPE RELATED TO APPROACH 1 IN COMPARISON WITH THE CONVENTIONAL MODEL (SIMULATION RESULTS)

Characteristics	Conventional	Optimal
η (%)	93.59	93.89
PF	0.904	0.899
I_{start} (A)	234.22	307.68
T_s (N.m)	339.82	401.45

B. Approach 2: Rotor slot shape

The shape of the slot is proportional to the leakage reactance of the slot which affects motor efficiency. Hence, in this approach, the rotor slot shape has been changed to investigate the effect of different slot shapes on motor performance characteristics considering constant slot area (134.2 mm²). The motor performance characteristics related to the conventional model and each rotor slot shapes (shown in Fig. 8) are presented in Tables 4. According to the results, the highest efficiency is 93.63 % in I, III, and IV prototypes. In these cases, the efficiency increases by 0.04 % in comparison with the efficiency of the conventional model.

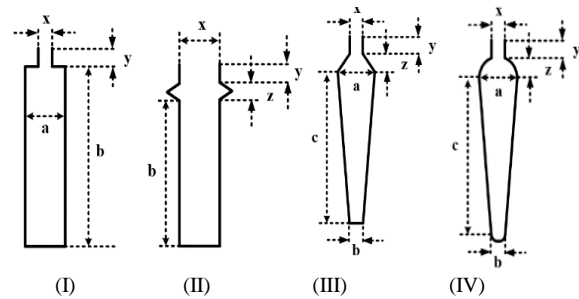


Fig.8. Five different prototypes of rotor slot shapes with the same area

TABLE IV
THE INDUCTION MOTOR PERFORMANCE CHARACTERISTICS RELATED TO APPROACH 2 BASED ON THE SHAPE IN COMPARISON WITH THE CONVENTIONAL MODEL (SIMULATION RESULTS)

Char.	Conv.	I	II	III	IV
η (%)	93.59	93.63	93.52	93.63	93.63
PF	0.904	0.918	0.876	0.912	0.912
I_{start} (A)	234.22	364.10	413.8	311.7	306.87
T_s (N.m)	339.82	512.72	647.66	472.74	468.72

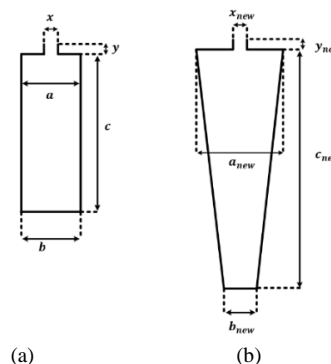


Fig.9. Rotor slot shape. (a)- Prototype I, (b)- Optimal model of prototype I

To optimize the presented prototypes of the rotor slot shape, the objective function considered maximum motor efficiency. Figure 9 shows the prototype and GA-based optimal shapes of the case I. In this optimal slot shape, the motor efficiency increased amount of 0.25%, and 0.2% in comparison with the conventional model (Fig. 2), and the prototype case I, respectively. Also, the efficiency in the GA-based optimal shape of case II (Fig. 10) increases by 0.21%, and 0.29% in comparison with the conventional model, and the prototype case II, respectively. Figures 11, and 12 show the prototype and GA-based optimal shapes of cases III, and IV, respectively. The efficiency of the optimal model in Fig. 11 increases by 0.32%, 0.28% in comparison with the conventional model, and the prototype case III, respectively. Also, the efficiency in the GA-based optimal shape of case IV (Fig. 12) increases by 0.31%, and 0.27% in comparison with the conventional model, and the prototype case IV, respectively. The efficiency results in all considered cases in this approach have been illustrated in Fig. 13. As mentioned before, the sensitivity analysis of the rotor slot dimensions showed that the suitable slot shape for higher efficiency is the slot with a tight top, and bottom width, wide middle width, and deep depth. The results of the GA validate the sensitivity analysis results.

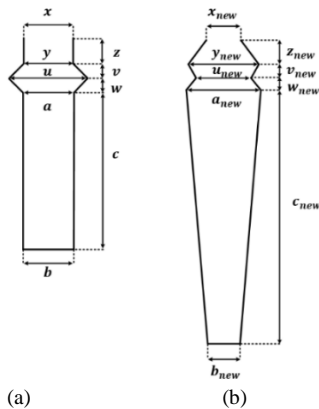


Fig.10. Rotor slot shape. (a)- Prototype II, (b)- Optimal model of prototype II

C. Approach 3: Stator and rotor diameters

1) changing of the stator and rotor diameters simultaneously

In this section, the objective function is maximum efficiency with considering four variables include D_{out-s} , D_{in-s} , D_{out-r} , D_{in-r} whereas the shape and dimensions of rotor and stator slots remain as same as the conventional model. The linear constraints are expressed as follow:

$$D_{out-s} - D_{in-s} > 2l_{slot-s} \quad (13)$$

$$D_{in-s} - D_{out-r} > 2l_g \quad (14)$$

$$D_{out-r} - D_{in-r} > l_{slot-r} + l_{er} \quad (15)$$

where l_{slot-s} is depth of stator slot, l_{slot-r} is depth of rotor slot, and l_{er} is end-ring width.

The limits of the design variable and the results of the optimization algorithm is presented in Tables 5 and 6 respectively. The results show that the optimal motor volume

is expanded by about 58% in comparison with the conventional model. Also, the efficiency in the optimal motor is 94.1% which increased by 0.55% in comparison with the conventional model. Besides, the starting torque and power factor in the optimal motor have been almost constant.

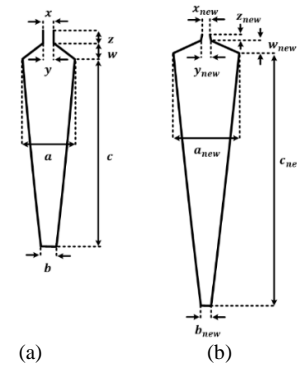


Fig.11. Rotor slot shape. (a)- Prototype III, (b)- Optimal model of prototype III

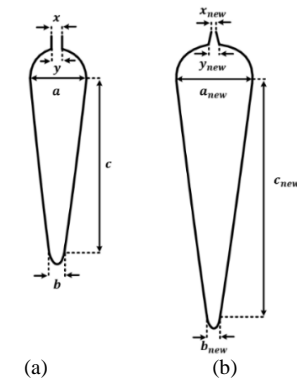


Fig.12. Rotor slot shape. (a)- Prototype IV, (b)- Optimal model of prototype IV

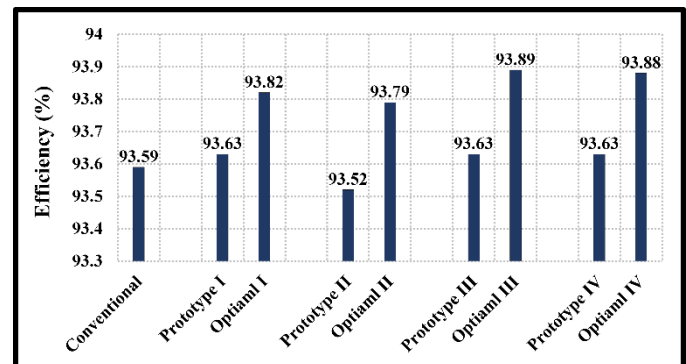


Fig.13. Comparison efficiency between prototype and optimal shape of slots related to the approach 2

2) changing of the stator outer diameter

In this section, if three variables include D_{in-s} , D_{out-r} , and D_{in-r} have been considered constant whereas D_{out-s} is changed as $2l_{slot-s} < D_{out-s} \leq 650\text{mm}$ based on the sensitivity analysis results in section 4.3, the highest efficiency is 94.3%. In this efficiency, D_{out-s} is 650mm and also the efficiency is increased by 0.76% in comparison with the efficiency of the conventional model. In general, when the motor core become larger, the flux density, as well as the core loss is decreased and the efficiency is increased consequently. The results of

this investigation are summarized in Table 7. According to the results, the starting torque and power factor have been almost constant similar to the changing of the stator and rotor diameters simultaneously.

TABLE V

THE OPTIMAL DIAMETERS OF THE STATOR AND ROTOR RELATED TO APPROACH 3 (THE STATOR AND ROTOR DIAMETERS) IN COMPARISON WITH THE CONVENTIONAL MODEL

Diameters (mm)	Conventional	Limits	Optimal
D_{out-s}	327	163.5-490.5	411.1
D_{in-s}	210	105-315	208.4
D_{out-r}	208.7	104.35-313.05	207.1
D_{in-r}	72	36-108	96.9

TABLE VI

THE INDUCTION MOTOR PERFORMANCE CHARACTERISTICS OF OPTIMAL MODEL RELATED TO APPROACH 3-A IN COMPARISON WITH THE CONVENTIONAL MODEL (SIMULATION RESULTS)

Characteristics	Conventional	Optimal
η (%)	93.59	94.1
PF	0.904	0.902
I_{start} (A)	234.22	235.12
T_s (N.m)	339.82	342

TABLE VII

THE INDUCTION MOTOR PERFORMANCE CHARACTERISTICS OF THE STATOR OUTER DIAMETERS VARIATIONS RELATED TO APPROACH 3-B (SIMULATION RESULTS)

Characteristics	Conventional	Optimal
η (%)	93.59	94.3
PF	0.904	0.905
I_{start} (A)	234.22	232.99
T_s (N.m)	339.82	336.59

D. Compare the results of considered approaches

In this paper, three considered approaches have been applied on a 30-kW set-up squirrel cage induction motor to analysis the motor performance characteristics. These approaches with a combination of the genetic algorithm lead to an optimal model for set-up induction motor. The performance characteristics of the optimal motor related to each approach are presented in Table 8. Based on the motor efficiency (Fig. 14), the approach 3-B leads to the highest motor efficiency (94.3%) between all considered approaches. The increase of efficiency in approaches 1, 2, 3-A, and 3-B in comparison with the efficiency of the conventional model are 0.32%, 0.32%, 0.55%, and 0.76%, respectively.

The important manufacturing considerations of the optimal motor in all presented approaches are summarized in Table 9. These considerations include stator slot mold, rotor slot mold, aluminum weight, shaft diameter, bearings, motor cortex, and cooling system. In approach 1, and 2 the rotor slot dimensions are changed as well as the rotor slot mold and aluminum weight. In approach 3-A, when the diameters of the rotor and stator are changed simultaneously, the slot mold of stator and rotor, shaft diameter, bearings, motor cortex, and cooling system is changed. However, in the approach 3-B, since the outer diameter of the stator is changed, only the stator slot mold and the cortex motor are changed.

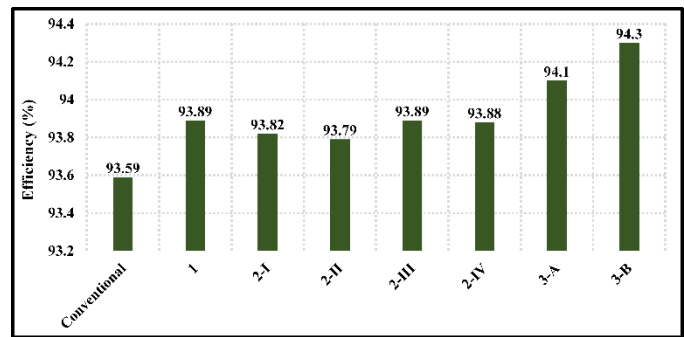


Fig.14. Comparison efficiency between considered approaches

TABLE VIII

THE INDUCTION MOTOR PERFORMANCE CHARACTERISTICS OF OPTIMAL MODEL RELATED TO THE CONSIDERED APPROACHES IN COMPARISON WITH THE CONVENTIONAL MODEL (SIMULATION RESULTS)

Characteristics	Conv.	App. 1	App. 2	App.3-A	App.3-B
η (%)	93.59	93.89	93.63	94.1	94.3
PF	0.904	0.899	0.912	0.902	0.905
I_{start} (A)	234.22	307.68	306.87	235.12	232.99
T_s (Nm)	339.82	401.45	468.72	342	336.59

TABLE IX

THE MANUFACTURING CONSIDERATIONS OF THE OPTIMAL MOTOR RELATED TO THE PRESENTED APPROACHES

Subject	App. 1	App. 2	App. 3-A	App. 4-B
Stator slot mold			✓	✓
Rotor slot mold	✓	✓	✓	
Aluminum weight	✓	✓		
Shaft diameter			✓	
Bearing			✓	
Motor cortex			✓	✓
Cooling system			✓	✓

In the approaches 1 and 2, due to the change in the dimensions of the rotor slot, in the process of producing the electromotor, the device that produces the rotor mold must be readjusted according to the new dimensions of the slot; However, this change in the dimensions of the rotor slot does not change the amount of material consumed by the rotor magnetic material. Also, due to the change in the dimensions of the slot, the amount of aluminum consumed in the rotor slots (rotor bars) increases, which will not cause problems in the production process and difficulties for electromotor manufacturers. In the approach 3, because all the geometric characteristics of the motor, including the rotor slot mold, stator slot mold, motor shaft, bearing and motor cortex are changed, it is necessary to adjust the molding machine for the rotor, as well as for the stator. Also, all parts must be re-machined, which increases the cost of production and operation of the devices. In addition, materials in the electromotor production increase, which increases motor costs. So, approach 3 is more difficult for the manufactures rather than approach 1 and 2. Also, the approach 4 due to the just changing in stator outer diameter is in a better position that the approach 3. In this approach the material consumption and motor cortex are changed. So, approach 1 and 2, Therefore, the approaches 1 and 2, then the approach 3 and then the approach 4 are considered from the lowest to the highest difficulty in the electromotor production process, respectively.

Thus, based on the motor efficiency and the manufacturing considerations, the optimal approach is approach 3-B. Hence,

the economic evaluation for this approach is accomplished in section 5.

VI. ECONOMIC EVALUATION

The simulation results obtained from four presented approaches in section 4 show that the starting torque increases in comparison with the conventional model. Although, the efficiency of the conventional motor is high so that it places into the IE2 group based on the IEC standard, however, in approach 4 the motor efficiency increases by 0.76 % in comparison with the conventional model. Although, the efficiency is increased by other approaches but the highest belongs to approach 4. In this approach, the stator iron part in the optimal model expand as well as the motor cost. So, the following economic evaluation has been employed to verify the optimal design of this approach [24].

The stator core price is calculated by specifying the net volume of the stator iron part. The core of 30-kW motor as a case study was made of sheets with grade m-470 which its price is 1.27 \$ per kilogram.

The volume of stator slots should be subtracted from the volume of the stator core. Now, the volume of the stator iron part (V_{iron}) is:

$$V_{iron} = (S_s - S_r - S_{slot})L \quad (16)$$

where S_s is the stator area, S_r is the rotor area, S_{slot} is the area of stator slots, and L is core length.

The stator core weight (W_s) is calculated using Eq. (17):

$$W_s = V_{iron} \sigma_{iron} \quad (17)$$

The price of stator core based on 1.27\$ per kilogram and motor energy losses in the conventional and optimal model related to approach 5 are presented in Table 10 and 11, respectively. The benefit of increased efficiency is calculated for three cases of electricity consumption cost include 0.0273\$ (case 1), 0.0655\$ (case 2), and 0.1\$ (case 3) per kWh. This benefit is calculated according to the energy losses per year and it is assumed that the motor is powered on continuously during the year. The results show that the total cost of the optimal motor related to the approach 5 has been increased by 637.913\$ in comparison with the conventional model due to an increase in stator core weight by about 435.7 kilograms.

This energy savings can be considered as an annual income (A) in the financial process. The residual value (F) of the motor after its useful life is considered to be 35 % of the initial value. Considering the time value of money, the number of interest periods (n) is determined using Eq. (18) [24].

$$-P(A/P, i\%, n) + A + F(A/F, i\%, n) = 0 \quad (18)$$

where P , F , A , and i are present worth, residual value, annual income, and interest rate, respectively. Also, the amount of $(A/P, i\%, n)$ and $(A/F, i\%, n)$ are determined in [25].

According to (18), the curves of the interest period number versus interest rates are depicted in Fig. 15 considering three cases for electricity consumption cost per kWh. As shown in this figure, the case 1 has no economic justification even at a low-interest rate. Regarding case 2, the results show that the optimal approach has economic justification for the interest

rate lower than 5% and also, case 3 has an economic justification for any interest rate. Thus, the optimal model extracted from approach 5 is an economical design if the electricity consumption cost per kWh is 0.1\$. Furthermore, if the time value of money is regardless of the financial process, the number of interest periods is 8.9, 3.71, and 2.43 years whereas the electricity consumption cost per kWh is 0.0273\$, 0.0655\$, and 0.1\$, respectively.

TABLE X
THE STATOR DIAMETER AND COST OF OPTIMAL MODEL RELATED TO APPROACH 5 IN COMPARISON WITH THE CONVENTIONAL MODEL

Parameters	Conventional	Optimal
D_{out-s} (mm)	327	650
L (mm)	230	230
W_s (kg)	70.1	508.8
C_s (\$)	88.073	647.576

TABLE XI
THE ENERGY AND COST OF LOSSES IN THE OPTIMAL MODEL RELATED TO APPROACH 5 IN COMPARISON WITH THE CONVENTIONAL MODEL FOR THREE CASES OF ELECTRICITY CONSUMPTION COST

Energy losses	Conventional	Optimal
η (%)	93.59	94.3
P_T (kW)	2.1	1.8
Energy losses (kWh) [for 1 year]	18396	15768
Energy losses cost (\$) [1 kWh = 0.0273\$]	501.71	430.04
Energy losses cost (\$) [1 kWh = 0.0655\$]	1204.10	1032.09
Energy losses cost (\$) [1 kWh = 0.1\$]	1839.6	1576.8

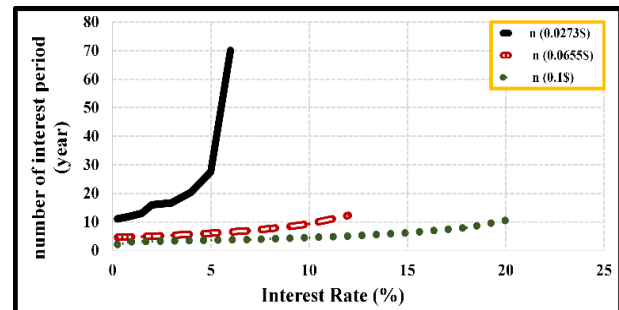


Fig.15. Number of interest period curves versus interest rates related to the economic evaluation for three cases of electricity consumption costs per kWh

VII. DISCUSSION

The performance characteristics of set-up induction motor have been calculated according to the mathematical equations in which they are proportional to the motor equivalent circuit. The simulated results extracted from Maxwell software are close to the analytical results as well as the experimental results.

In this article, the goal is the optimal efficiency design of induction motors. The sensitivity of the rotor slot dimensions showed that the rotor slot with the tight top and bottom parts and with the wide middle part has the highest efficiency. Also, the sensitivity of the stator and rotor diameters showed that the efficiency is increased significantly when the motor core is expanded. Hence, three different approaches have been applied on a 30-kW, 4-pole, 3-phase squirrel cage induction motor to improve the motor performance characteristics such as efficiency, and starting torque. These approaches include

design of rotor slot (Approach 1), rotor slot shape (Approach 2), stator and rotor diameters (Approach 3).

The genetic algorithm is employed to find the optimal model in each considered approach. The optimal motor efficiency in approaches 1, 2, 3-A, and 3-B are 93.89%, 93.89%, 94.1% and 94.3%. Finally, approach 3-B is chosen as the optimal design approach. The economic evaluation of this optimal motor design is accomplished for three different cases of electricity consumption costs. The optimal model has less energy loss than the conventional model. But in the optimal model, the price is higher since the stator diameter of the motor is larger. The results show that the additional cost of the optimal motor is returned during 4 years with an interest rate of 5%.

REFERENCES

- [1] Lee H. J., Im S.H., Um D. Y., Park G. S. (2018) A design of rotor bar for improving starting torque by analyzing rotor resistance and reactance in squirrel cage induction motor. *IEEE Trans Magn* 54(3)
- [2] Khelifi H., Hamdani S. (2019) Induction motor rotor fault diagnosis using three-phase current intersection signal. *Electr Eng*, <https://doi.org/10.1007/s00202-019-00894-7>
- [3] Parkash R., Akhtar M. J., Behra R. K., Parida S. K. (2014) Design of a three phase squirrel cage induction motor for electric propulsion systems. *Third International Conference on Advances in Control and Optimization of Dynamical Systems*, Kanpur, India
- [4] Oraee H. (2000) A quantitative approach to estimate the life expectancy of motor insulation systems. *IEEE Transaction on Dielectric and Electrical Insulation* 7(6): 790-796
- [5] Rengifo J., Alb'anez E., Benzaquen J. (2018) Full-load range in-situ efficiency estimation method for induction motors using only a direct start-up. *XIII International Conference on Electrical Machines (ICEM), Alexandroupoli, Greece*
- [6] Kim H. M., Lee K. W., Kim D.G., Park J. H., Park G. S. (2018) Design of cryogenic induction motor submerged in liquefied natural gas. *IEEE Trans Magn* 54(3)
- [7] Zhang D., Park C. S., Koh C. S. (2012) A new optimal design method of rotor slot of three-phase squirrel cage induction motor for NEMA class D speed-torque characteristic using multi-objective optimization algorithm. *IEEE Trans Magn* 48(2)
- [8] Lee D., Jung H. C. (2018) Cost pattern value method for local search algorithms applied to optimal FEA-based design of induction motors. *IEEE Trans Magn* 53(11)
- [9] Haisen Z., Jian Z., Xiangyu W., Qing W., Xiaofang L., Yingli L. (2014) A design method for cage induction motors with non-skewed rotor bars. *IEEE Trans Magn* 50(2)
- [10] Lee G., Min S., Hong J.P. (2013) Optimal shape design of rotor slot in squirrel-cage induction motor considering torque characteristics. *IEEE Trans Magn* 49(5), Vol. 49, No. 5, May, 2013.
- [11] Yetgin A. G. (2020) Investigation of the effects of stator slot permeance on induction motor and obtaining the best starting torque using permeance calculation. *Canadian Journal of Electrical And Computer Engineering* 43(1): 25-29
- [12] Yun J., Lee S. B. (2018) Influence of aluminum die-cast rotor porosity on the efficiency of induction machines. *IEEE Trans Magn* 54(11)
- [13] Yun J., Lee S., Jeong M., Lee S. B. (2018) Influence of die cast rotor fill factor on the starting performance of induction machines. *IEEE Trans Magn* 54(3)
- [14] Kim D. J., Jung J. W., Hong J.P., Kim K.J., Park C.J. (2012) A study on the design process of noise reduction in induction motors. *IEEE Trans Magn* 48(11)
- [15] Wang L., Bao X., Di C., Li J. (2015) Effects of novel skewed rotor in squirrel-cage induction motor on electromagnetic force. *IEEE Trans Magn* 51(11)
- [16] Heo C. G., Kim H. M., Park G. S. (2017) A design of rotor bar inclination in squirrel cage induction machines. *IEEE Trans Magn* 51(11)
- [17] Zhang D., Park C. S., Koh C. S. (2012) A novel method for multi-objective design and optimization of three phase induction machines. *IEEE Trans Magn* 48(2)
- [18] Zhang D., Park C. S., Koh C. S. (2019) Design optimization of wound rotor induction motor using genetic algorithm. *5th Conference on Knowledge-Based Engineering and Innovation*, Tehran, Iran
- [19] Agamloh E. B., Boglietti A., Cavagnino A. (2013) The incremental design efficiency improvement of commercially manufactured induction motors. *IEEE Transaction on Ind Appl* 49(6): 2496 – 2504
- [20] Mallik S., Mallik K., Barman A., Maiti D., Biswas S. K., Deb N. K., Basu S. (2017) Efficiency and cost optimized design of an induction motor using genetic algorithm. *IEEE Trans Ind Elect* 64(12): 9854-9863
- [21] Boldea I., Nasar S. A. (2010) *The induction machines design handbook*. 2nd edition, CRC Press, USA.
- [22] Haque M. (2008) Determination of NEMA design induction motor parameters from manufacture data. *IEEE Trans Energy Conv* 23(4): 997-1004
- [23] Rengifo J., Romero J. (2018) Efficiency evaluation of induction motors supplied by VFDs. *IEEE Third Ecuador Technical Chapters Meeting (ETCM)*, Cuenca, Ecuador.
- [24] Varghese T., Rajagopal R. (2016) Economic and efficient induction motor controller for electric vehicle using improved scalar algorithm. *1st IEEE International Conference on Power Electronics, Intelligent Control and Energy Systems (ICPEICES)*, Delhi, India
- [25] Oskounejad M. M. (1996) *Economic engineering, economic evaluation of industrial projects*. 7th edition, Publishing center of Amirkabir university: CRC Press, Iran

BIOGRAPHIES



Mahdi Rezaiee Nakhaie was born in Kashmar, Iran, in 1994. He received the B.Sc. degree in power electrical engineering from Hakim Sabzevari University (HSU), Sabzevar, Iran in 2017, where also he is received the M.Sc. degree in HSU. His research interest is design of electrical machines, power system.



Reza Roshanfekar was born in Sabzevar, Iran, in 1980. He received the B.Sc. degree in power electrical engineering from Amirkabir University (AKU), Tehran, Iran in 2002, and the M.Sc. and Ph.D. degree from Iran University of Science and Technology (IUST), Tehran, Iran, in 2004 and 2017, respectively. He joined the electrical Group of the Department of Electrical Engineering at Hakim Sabzevari University in 2006, where he is Assistant Professor. His research interests are fault diagnosis in electrical machines, design of electrical machines, and power quality.